J|A|C|S ARTICLES

Published on Web 01/06/2009

The Oil−Water Interface: Mapping the Solvation Potential

Richard C. Bell,*,† Kai Wu,‡ Martin J. Iedema,§ Gregory K. Schenter,§ and James P. Cowin*,§

Chemistry Department, The Pennsylvania State University, Altoona College, Altoona, Pennsylvania 16601, Beijing National Laboratory for Molecular Sciences, College of Chemistry and Molecular Engineering, Peking University, Beijing 100871, China, and Pacific Northwest National Laboratory, K8-88, Richland, Washington 99354

Received July 30, 2008; E-mail: jp.cowin@pnl.gov

Abstract: An ion moving across an oil−water interface experiences strong solvation changes. We have directly measured the solvation potential from 0.4 to 4 nm for Cs^+ ions approaching the oil−water interface from the oil side ("oil" = 3-methylpentane). The interfaces were built at 30 K using molecular beam epitaxy. Ions were precisely placed within the film during its growth using a soft-landing ion beam. The ion's *collective* electric field was progressively increased (by adding more ions) until it balanced the *individual* ion's solvation potential slope. As the samples were slowly warmed, near 90 K the ions began moving, as measured by a Kelvin probe. Their motion precisely determines the local slope of the solvation potential, which was integrated to get the potential. The potential is Born-like for $z > 0.4$ nm away from the oil−water interface. Our method could provide important tests of theoretical estimates of ion motion at biological interfaces and in atmospheric aerosols.

There are many biological and chemical reactions involving transport across interfaces between two immiscible phases. Ions moving across an oil−water interface are strongly impacted by the continuous changes in solvation as they traverse the interface.[1] Similar variations exist near the junction of water and any substance with a low dielectric permittivity (air, oil, cell membranes, proteins, etc.). This leads to gross changes in the ion's energetics and kinetics and in the interfacial equilibrium ion concentrations. Simplistic models (i.e., the Born model)[2] have given way to recent advances in computational methods.[1,3] Correspondingly, direct experimental probes of the solvation potential have been few and usually indirect.[4,5]

In contrast, we are able to nonperturbatively probe the ion potentials at the water−oil interface in a manner that is free of many of the complicating factors (such as counterions and mechanical probes) associated with many other techniques. Here we define the solvation potential as the average chemical potential that a single ion experiences at a given distance from the interface. Figure 1 shows (as the heavy black-and-gray line) the solvation chemical potential that we determined in this work: that for a single ion approaching an 18 Å [4.4 monolayer (ML)] film of water (shaded blue) immersed in 3-methylpentane (3MP) (shaded tan). To the far left is a metallic substrate (shaded gray).

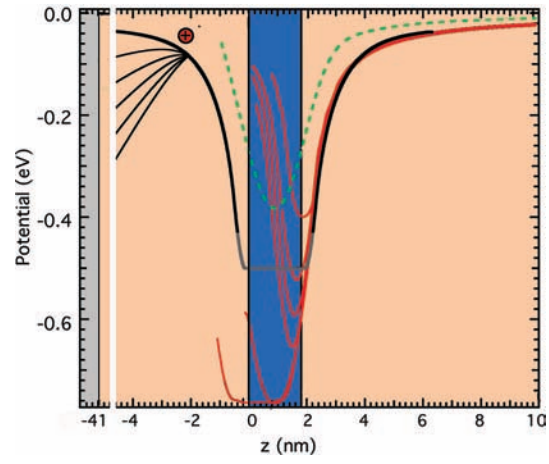

Figure 1. Solvation chemical potential for a single ion (heavy black-and-gray line) traversing a 1.8 nm (4.4 ML) water layer (blue region) within a 3MP film (tan region) sitting on a metal substrate (gray region) located 41 nm from the left interface (i.e., at $z = -41$ nm). The black portion of the potential curve was directly measured here, and the well depth (gray portion) was inferred in ref 6. The thin black curves at the left show the solvation potential plus the collective potential generated by ions placed 5 ML (2.1 nm) from the left side of the water film, to create electric fields of 2, 4, 6, 8, and 10×10^7 V/m. The red curves are Born calculations for $r_b = 5$ Å, $\varepsilon_1 = 1.9$, $\varepsilon_2 = 100$, and water films with thicknesses of 0.15, 0.3, 0.45, 0.6, 1.8, and 3.0 nm (lined up on the right side). The green dashed curve is the Born model for a 1.8 nm water film with $\varepsilon_2 = 5$.

In a previous work,[6] we estimated the well depth of the solvation potential as a function of the thickness of the water film, using the measured temperature at which ions escaped the bottom of the solvation potential while the temperature of the film was slowly increased. Those well depths were in fair agreement with

† Pennsylvania State University, Altoona.
‡ Peking University.
§ Pacific Northwest National Laboratory.

(1) Hofft, O.; Borodin, A.; Kahnert, U.; Kempter, V.; Dang, L. X.; Jungwirth, P. *J. Phys. Chem. B* **2006**, *110*, 11971–11976.
(2) Born, M. *Z. Phys.* **1920**, *1*, 45–48.
(3) Chang, T.; Dang, L. X. *Chem. Rev.* **2006**, *106*, 1305–1322.
(4) Mulkidjanian, A. Y.; Cherepanov, D. A. *Photochem. Photobiol. Sci.* **2006**, *5*, 577–587.
(5) Mulkidjanian, A. Y.; Herberle, J.; Cherepanov, D. A. *Biochim. Biophys. Acta* **2006**, *1757*, 913–930.
(6) Wu, K.; Iedema, M. J.; Cowin, J. P. *Science* **1999**, *286*, 2482–2485.

the ones predicted by the Born potential and depended strongly on the water film thickness (for thicknesses <10 ML). The Born model treats the oil and water as smooth dielectrics with dielectric constants ε_1 (~1.9 for 3MP) and ε_2, respectively. The ion is treated as a point charge q_e in a hollow sphere of radius r_b. The predicted well depth for moving a Born ion from the oil to the water in the limit of a very thick water film is given by $(1/\varepsilon_1 - 1/\varepsilon_2)q_e/8\pi\varepsilon_0 r_b$, where ε_0 is the vacuum permittivity. For the simulations presented here, a single ε_2 value of 5 and an r_b value of 6 Å reasonably fit the well depth as a function of water film thickness. A potential for nearly this case (but with $r_b = 5$ Å) is shown in Figure 1 as the dashed green curve.

The enhanced mobility expected within such a thin water film compared with that within bulk ice should permit the dielectric constant of the water films to be fully active at temperatures at which the ions escape (90−150 K). This would imply that ε_2 should be roughly between 150 and 200. Thus, the fact that the "effective" ε_2 required to fit the well-depth data is on the order of 5 indicates that, at least very near the solvated ions, there is an inability of the water molecules to reorient with the spatial resolution implied by the simple continuum model.[7] This same effect is well-known in electrochemical double layers, where water within a monolayer or two of the electrode has an effective dielectric permittivity on the order of 4 to 6.[7,8] This is sometimes expressed in terms of a "*k*-dependent" dielectric constant, where *k* is determined from the Fourier transform of the spatial distribution of the induced charges, which is required to understand solvation in liquid water and its interfaces.[7]

The estimate of the well depth[6] had several shortcomings: (1) The ions escaped at fairly high temperatures (95−150 K), where the rapidly increasing mobility of the water molecules could permit gross rearrangement of the water layers from their initial geometry, in response to the field around a single ion. This may have caused the water film to thicken around each ion. (2) A simple-minded one-dimensional well was used in the analysis, with an assumed pre-exponential factor for the phenomenological Arrhenius kinetics of ion escape from the water layer. (3) The escape of the ions from the water layer was accompanied by damage to the water film that actually destroyed the films' continuous nature.[6] The film destruction was thought to be caused by dewetting, whereby the escaping ions tore holes in the water film. This eliminated the surface-tension energy barrier that prevents the planar water films from turning into large water droplets/crystals.

Experimental Section

In this study, we mapped this solvation potential in detail, eliminating the limitations of the earlier well-depth experiments. The "oil" films of 3MP with embedded water layers were prepared via molecular beam epitaxy at low temperatures (~30 K).[9] 3MP is an excellent glass, as it never crystallizes and becomes progressively more fluid above its glass transition temperature of 77 K. We placed small amounts of Cs^+ ions into the "oil" at carefully determined distances from the oil−water interface. By exploring the motion of these ions as the film was warmed above its glass temperature, we determined the precise slope of the chemical solvation potential as a function of distance from the interface, which was then integrated to obtain the potential. A Kelvin probe measured the ion motion via the total work function change. The ions in the dielectric act like a simple capacitor, producing a film voltage V_f that is directly proportional to the average vertical position of the ions within the 3MP. Since the total film voltage was on the order of 10 V for a 100 ML film and could be measured to better than 0.01 V, this implies that average ion motions of $^1/_{10}$ of a monolayer could be readily detected.

Apparatus and Sample Preparation. The films were deposited using a molecular beam, and the ions were deposited using an ion soft-landing approach in an ultrahigh vacuum apparatus with a base pressure of 2×10^{-10} Torr. The details of the experimental procedures have been reported previously,[10,12,13] so only a brief overview is reported herein. The organic films were epitaxially deposited onto a 1 cm diameter Pt(111) substrate using a four-stage differentially pumped molecular beam. The second step involved the gentle deposition of Cs^+ ions on the film. The ion beam energy was less than 1 eV. Similarly, hydronium (D_3O^+) ions could be deposited. If ions were to be placed inside a film, the film was deposited first up to the thickness where the ions were to be placed, and then the ions were deposited. Additional layers of 3MP and/or water were then deposited on top of the ions. Finally, the voltage across the film (which is related to the average vertical position of the ions within the film) was measured nonperturbatively using a Kelvin probe. This was done while the temperature was increased at a constant rate (0.2 K/s for these studies). The films began to significantly evaporate at 120−140 K, which was well above the temperature at which the ions had fully traversed the film. The thermal desorption of the film was monitored with a mass spectrometer.

The Pt(111) substrate was cleaned by sputtering with neon ions followed by annealing at 1030 K in a 1×10^{-7} Torr oxygen atmosphere. Finally, the substrate was annealed to 1200 K in vacuum. The cleanliness of the substrate surface was monitored using Auger electron spectroscopy. The sample was cooled to below 30 K using a closed-cycle helium refrigerator and radiatively heated by an array of tungsten filaments located behind the substrate. They were biased slightly positively to prevent electron emission. The temperature was measured by a K-type thermocouple (Ni−Cr/Ni−Al) spot-welded to the sides of the platinum substrate. 3MP (which does not crystallize[14]) was purified by freeze−pump−thaw treatments under vacuum. Molecular sieve was used to remove any possible water contamination, with the purity of the vapor checked with a mass spectrometer. All film layer thicknesses are reported as multiples of a nominal monolayer, with 1 ML being just what is required to saturate the most tightly bound thermal desorption peak. Through the use of reflectance techniques and thermal desorption studies, the deposition rate of the molecular beam was established from the thickness of the films at a given deposition time.[10] The deposition rate used for these studies was 8.5 s per nominal ML. The reflectance measurements showed that this was 0.49 Å/s, which corresponds to 4.2 Å per ML for 3MP.

The Cs^+ ions were generated using a thermionic button source[15] and then extracted and transmitted at 300−400 eV by electrostatic optics and deflectors through two 5° bends along the ion path. These bends, along with several liquid nitrogen traps and differential pumping, suppressed contamination by water or other possible contaminants during ion deposition to less than 1% of the ion flux. A Wien filter (with perpendicular electric and magnetic fields) was used to mass-select the ion of interest. The ions were decelerated to less than 1 eV as they passed through a grounded double mesh

(7) Hildebrandt, A.; Blossey, R.; Rjasanow, S.; Kohlbacher, O.; Lenhof, H.-P. *Phys. Rev. Lett.* **2004**, *93*, 108104, and references therein.
(8) Bockris, J. O.; Reddy, A. K. N. *Modern Electrochemistry*; Plenum Press: New York, 1977.
(9) Wu, K.; Iedema, M. J.; Schenter, G. K.; Cowin, J. P. *J. Phys. Chem. B* **2001**, *105*, 2483–2498.
(10) Bell, R. C.; Wu, K.; Iedema, M. J.; Cowin, J. P. *J. Chem. Phys.* **2007**, *127*, 024704.
(11) Bell, R. C.; Wang, H.; Iedema, M. J.; Cowin, J. P. *J. Am. Chem. Soc.* **2003**, *125*, 5176–5185.
(12) Biesecker, J. P.; Ellison, G. B.; Wang, H.; Iedema, M. J.; Tsekouras, A. A.; Cowin, J. P. *Rev. Sci. Instrum.* **1998**, *69*, 485–495.
(13) Tsekouras, A. A.; Iedema, M. J.; Ellison, G. B.; Cowin, J. P. *Int. J. Mass Spectrom. Ion Processes* **1998**, *174*, 219–230.
(14) Finke, H. L.; Messerly, J. F. *J. Chem. Thermodyn.* **1973**, *5*, 247–257.
(15) HeatWave Labs, Inc. (Watsonville, CA), model 1139−01.

located ~1 cm away from the sample. Biasing the sample allowed the deposition energy of the ions to be regulated to ~1 eV. During ion deposition, the current of the impinging ions was recorded. In this manner, the total charge was calculated by integrating the ion current over the deposition period. The total ion coverages used in this study varied from near zero to ~0.05% of the surface density of the Pt(111) substrate (1.5×10^{15} ions/cm^2). The exact ion density was chosen to achieve the desired electric field. All of the ion depositions were carried out below 30 K in this study.

The deposited ions generate a collective voltage across the film. The organic film acts like a linear dielectric insulator, creating a planar capacitor in which the ions act to charge the capacitor. The capacitance of the system is $C = Q/V$, where V is the potential difference across the capacitor and Q is the total charge of the deposited ions. The capacitance can also be represented as $C = \varepsilon_0\varepsilon A/L$, where ε_0 is the vacuum permittivity, ε is the dielectric constant of the deposited film, A is the area of the plate (the Pt substrate), and L is the distance between the plates of the capacitor. Combining these two equations gives $V = QL/\varepsilon_0\varepsilon A$. Once the ions begin to traverse the film, they begin to spread out along the z direction (perpendicular to the two plates). The above equation is still valid for a uniform composition film, if L is replaced with the average height of the ions from the metal substrate, $\langle z \rangle$. The work function ϕ of the combined metal and film assembly is changed by the positions of the ions in the film by an amount $\Delta\phi$:

$$\Delta\phi = -\frac{Q\langle z\rangle}{\varepsilon_0\varepsilon A} = -\Delta V \tag{1}$$

where ΔV is the voltage across the film, which will be called the film voltage, V_f.

A McAllister Kelvin probe[16] with a sensitivity and measurement error of several millivolts was used to measure the film voltages. The probe tip was a 3 mm diameter, slightly domed mesh that was gold-plated. It was positioned ~0.5 mm away from the substrate and vibrated toward and away from the sample by a fraction of a millimeter at a frequency ω (a few hundred Hz). It was maintained at a relative voltage bias with respect to the sample. Its mutual capacitance with the area of the sample causes a purely alternating current to flow whenever there is any net potential difference between the vacuum just outside the edge of the sample and the probe. The Kelvin probe controller automatically adjusts the probe with the voltage bias to make this alternating current zero. This required bias is the "contact potential difference" (CPD) between the sample and the probe. This CPD equals $-\Delta\Phi = \Phi_{probe} - \Phi_{sample}$, where Φ_{probe} and Φ_{sample} are the work functions of the probe and the sample, respectively. Positive ions in the sample's dielectric film create a positive V_f by reducing the sample work function.

The change in the film voltage was monitored as the sample was warmed at 0.2 K/s (typically); thereby tracking the average position of the ions within the film. The He refrigerator was turned off during this time to prevent noise from mechanical vibrations during the measurement process. The molecular epitaxy caused a very slight and very reproducible alignment of the 3MP molecules when they were deposited well below the glass temperature of 3MP, creating weak electrets or ferroelectric film (a voltage across the film).[10,17,18] This is due to the slight dipole of 3MP. This voltage (8 mV/ML for deposition at 30 K) could be completely removed by annealing the film to above the glass temperature. If the film was not preannealed, this ferroelectric voltage disappeared just above the glass temperature and just before the bulk of the ions began to move. In this study, the ferroelectric voltage for the 3MP below the ions was preannealed, but the 3MP added on top could not be. To correct for the slight voltage change due to the unannealed portion of the film, identical films without ions were generated, and voltage versus temperature change data were measured. These data were subtracted from the case with ions present. Ion motion in annealed or nonannealed films appeared to be identical, and the ferroelectric voltages were very reproducible, allowing them to be easily recognized and easily removed by subtraction of the data for the films without ions present.[10]

Modeling of Ion Motion. The film voltage is a direct measure of ion position and thus of ion mobility within the total potential. The ions' motion through the film was modeled by calculating the time evolution of the ion distribution $\rho(z)$ of positive ions of charge nq_e using the diffusion equation with a term added to account for mobility within the electric field, as follows:

$$\frac{d\rho(z)}{dt} = \frac{d}{dz}D(z)\frac{d\rho(z)}{dz} - \frac{d[\mu(z)\rho(z)E_z(z)]}{dz} \tag{2}$$

The first term on the right side of eq 2 addresses the thermal random-walk motion of the particles, as described by the diffusion coefficient, D, while the second term models the ion mobility, μ, driven by an external electric field E_z. In the above equation, D and μ are allowed to vary in the z direction. The diffusion coefficient and the ion mobility are linked by the Einstein relation $D = \mu k_B T/nq_e$,[19] in which k_B is Boltzmann's constant.

Equation 2 was numerically propagated in time by the very stable implicit matrix approach.[20] The model of the film was divided into 5000 to 10 000 slabs, and time steps of 0.1 s were used for computational purposes. The bulk ion mobility is discussed in detail in refs 10 and 11. In this later study, it was shown that there are large, short-range (<10 ML) perturbations in the mobility of the ions near both the vacuum− and solid−liquid interfaces. In the present study, the ions were placed far enough from the vacuum interface to avoid this. By comparing the ion motion for ions placed just above the water versus just below it, we did see evidence suggesting changes in mobility (at a lesser level) near the oil−water interface. These "titration-like" experiments are largely insensitive to this effect, and it was not included in the simulations performed here.

Results and Discussion

Figure 2 shows the normalized film voltage (i.e., the measured film voltage divided by the initial film voltage) for each of a series of composite films in which ~$^1/_{1000}$ of a monolayer of Cs^+ ions was initially placed upon a 100 ML 3MP film, followed by an additional 2 ML of 3MP at 30 K and then a capping 0, 2, 5, or 10 ML water film; then the film was slowly warmed at 0.2 K/s. In our earlier experiments, the 3MP spacer layer was omitted.[6] For 0 ML of water, all of the ions move to the Pt substrate within a few degrees of becoming mobile near 90 K, as a result of the image potential created by their collective electric field, as the viscosity decreases and the ion mobility increases rapidly with temperature. This causes the film voltage to drop to zero near 90 K. For 2 to 10 ML of water, the voltage shows an initial partial drop near 90 K (as discussed below). However, the most striking feature is that a large portion of the ions become trapped at the oil−water interface by the solvation potential. The ions that are trapped are not expected to simply remain at their initial position in the 3MP but instead are expected to find their way to the water layer itself. Eventually they thermally escape the trap, at 98, 132, and 152 K from the 2, 5, and 10 ML water layers, respectively. Previously, this

(16) McAllister Technical Services (Coeur d'Alene, ID), model 6500.
(17) Iedema, M. J.; Dresser, M. J.; Doering, D. L.; Rowland, J. B.; Hess, W. P.; Tsekouras, A. A.; Cowin, J. P. *J. Phys. Chem. B* **1998**, *102*, 9203–9214.
(18) Wu, K.; Iedema, M. J.; Tsekouras, A. A.; Cowin, J. P. *Nucl. Instrum. Methods Phys. Res., Sect. B* **1999**, *157*, 259–269.
(19) Atkins, P. W. *Physical Chemistry*, 4th ed.; W. H. Freeman and Company: New York, 1990; p 764.
(20) Incropera, F. P.; DeWitt, D. P. *Fundamentals of Heat and Mass Transfer*, 4th ed; John Wiley & Sons: New York, 1996.

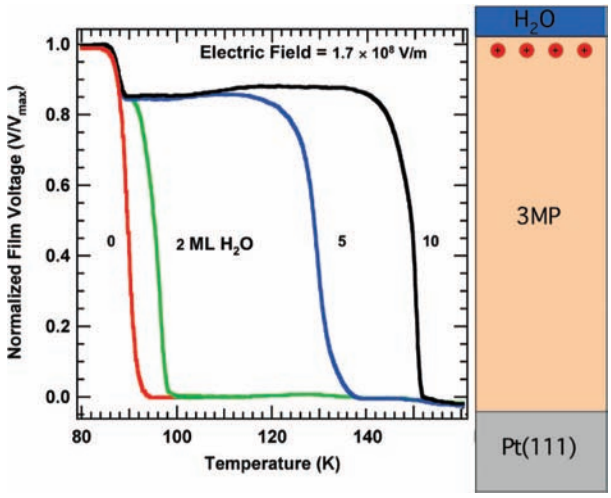

Figure 2. Normalized film voltage versus T (for a 0.2 K/s ramp) for composite films (diagram at right). The ions were initially placed on a 100 ML 3MP film, followed by an additional 2 ML of 3MP at 30 K and then a capping 0, 2, 5, or 10 ML water film. The 15% drop near 90 K in the case of the 2, 5, and 10 ML water films indicates that 15% of the ions initially escape the water trap (independent of water film thickness). The trapped ions escape at 95, 134, and 150 K for progressively thicker water films.

escape temperature along with the electrostatic potential of the ions' collective electric field with no 3MP spacer layer was used to estimate the well depths.[6] Here, as in the previous study, the well depth varied rapidly with water film thickness until finally saturating near 10−12 ML of water. Our focus here is the number of ions that become trapped, not their eventual escape.

The initial voltage drop near 90 K corresponds to ∼15% of the ions escaping the solvation potential when they are 2 ML away from the interface and reaching the Pt, while the remaining 85% become trapped within this solvation potential. The fraction of ions that are initially trapped tells much about the slope of the solvation potential at that initial location. Ions placed within the film alter the solvation potential as a result of the added electric potential that the ions collectively produce, as shown on the left side of Figure 1. For very few ions, the solvation potential is unchanged from the heavy black curve. In the case of a few ions, as long as the ions are several k_BT below the top of the well, they are all trapped in the solvation potential and migrate to the water layer (as shown in Figure 1 with the initial ion position marked with the red dot). However, as the number of ions increases, the net potential begins to bend downward, eventually reaching (and exceeding) zero slope at the initial ion position. When the number of ions is sufficient to locally bend the potential to have zero slope, the ion motion is profoundly altered.

Continuum numerical simulations were performed to show how the ion motion might be altered by this collective potential in the presence of the solvation potential. The ion's interaction with the water film was assumed to be the thick black-and-gray curve in Figure 1. The right-hand side of Figure 3 shows the ion motion predicted for ions in the net potential (i.e., the solvation potential plus the collective electrostatic potential generated by the ions), initially 2 ML below a 2 ML thick water film, using the ion mobility measured for this system as a function of T.[10] The solvation potential used was nearly the same as that shown in Figure 1 (see below). For a small number of ions (i.e., a small initial V_f), all of the ions are initially predicted to be trapped. As the initial V_f increases, the escape of some of the ions is evident by the drop in $V_f(T)$ near 90 K and the eventual voltage plateau that corresponds to the number of trapped ions. It is striking that as the initial V_f is increased by doping in more and more ions, there is an asymptotic amount of charge (number of ions) that can be trapped, here yielding a voltage plateau slightly over 6 V. This corresponds closely to that charge needed to bend the solvation potential at the ions' initial position enough to have zero slope, thus allowing any additional ions to escape without a barrier. This asymptotic limit is shown by the horizontal line in Figure 3. We also see that if the initial film voltage is higher than the final trapped voltage by ∼25% or more, then this final trapped voltage is near the maximum possible. This implies that the maximum amount of trapped charge (determined from the voltage of trapped ions) is a direct measure of the slope of the solvation potential at that distance.

The experimental results for ions initially 2 ML below a 2 ML thick water film are shown to the left in Figure 3. As predicted for small numbers of ions, nearly all of the ions are trapped. For an increasing number of ions, the amount of trapped ions reaches an asymptotic limit (proportional to the 7.3 V asymptote). This voltage divided by the distance to the Pt (100 ML = 42 nm) yields the slope of the solvation potential 2 ML away from the oil−water interface. The escape of ions at higher temperatures (≥95 K) looks quite different than predicted by theory. This difference is a result of the destruction of the water film by the escaping ions but does not change the conclusion about what the 90 K motion measures, as the film was intact at that temperature.

Similar experiments were performed for films in which the ions were placed from 1 to 10 ML away from the water layer, with water layers ranging from 2 to 30 ML thick. One initially surprising result (though consistent with simulations, as shown later) was the fact that the determined slopes of the solvation potential were independent of the water film thickness. This thickness independence is seen in Figure 2. There 15% of the ions escape, independent of the thickness of the water film, even though the well depth deduced from the escape temperatures varies rapidly with the water film thickness.

Figure 4 shows the trapped voltages versus distance from the water film for a variety of water film thicknesses from 2 to 30 ML and many initial film voltages. In Figure 4, those data for initial voltages that were at least 25% greater than the final trapped voltage are shown as large dots, while the rest are shown as small dots. To clearly display the large number of closely clustered data points, some of the results were plotted over a small range of ±0.3 ML. The large points were fit with a single exponential plus a $1/L^2$ gradient, where L is the distance of the ion to the nearest surface of the water film. The fit was done without the pictorial lateral spread in the points. This fit the data fairly well. The functional form was for numerical convenience and is not meant to imply a physical model. The fitted function is proportional to the slope of the solvation potential, and the right axis shows it in those units. When all of the data points in the figure are used, and not just the ones fully at the asymptotic limit, one gets a slightly different potential, which was the one used in the theoretical estimates for the right side of Figure 3. This is why the asymptotes in the right- and left-hand sides of Figure 3 are a little different. Only the fully asymptotic data is used in the remainder of the paper.

Integration of the fitted slope function gives the experimentally determined solvation potential. We know this potential should go to zero at large distances, but we do not have data

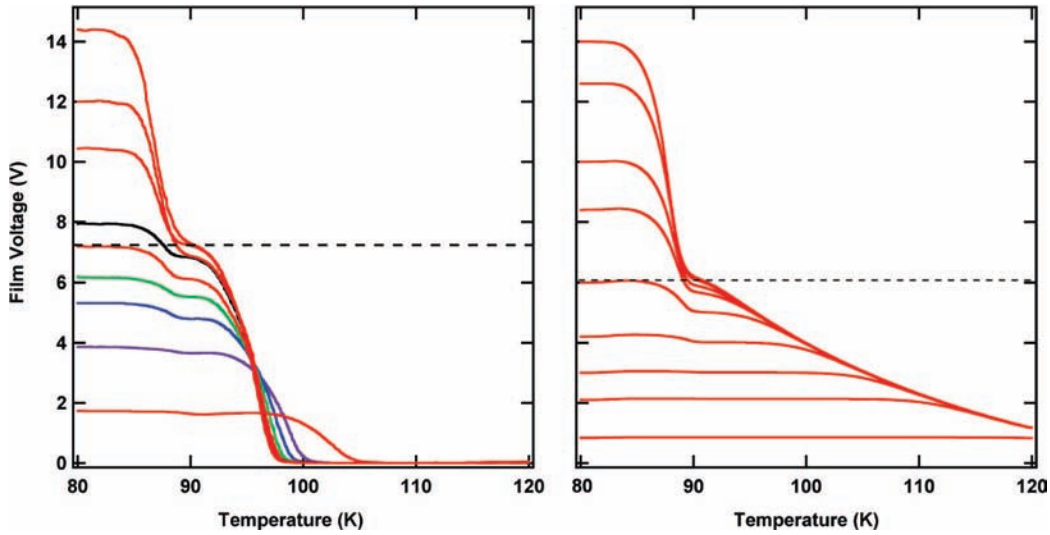

Figure 3. (left) Experimental and (right) simulated film voltage versus temperature results for placing ions 2 ML below a 2 ML thick water layer at 30 K and then warming at 0.2 K/s. The simulated results use a well and well depth that is almost the same as that shown by the heavy black-and-gray line in Figure 1 (see text) and assume that the ion mobility and diffusivity are continuum-like. The asymptotic limit of the shoulder near 90 K (i.e., of the "trapped" voltage) divided by the film thickness gives the slope of the solvation potential 2 ML from the water layer.

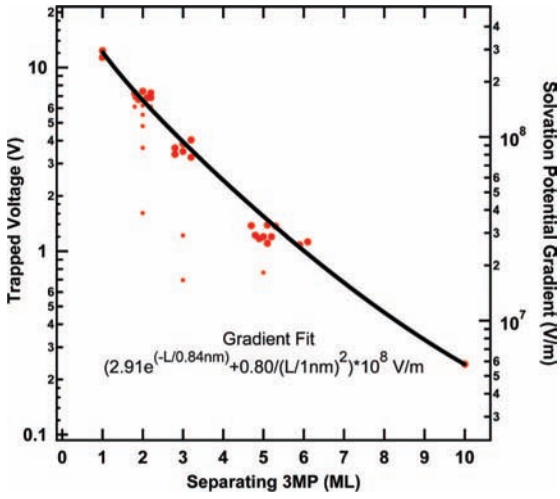

Figure 4. Trapped voltage (the shoulder near 90 K for experiments like that in Figure 3) plotted vs the distance L from the water layer, for water layer thickness varying from 2 to 30 ML. The larger points are ones for which the starting voltage was larger than 1.25 times the trapped voltage and are the only ones used for the fitted expression. These give the solvation potential slope, as shown on the right axis. The lateral scatter in the data for nominal coverages of 2, 3, 5, and 6 ML is for illustration only.

beyond 30 ML. Integration of the extrapolated functional form (an exponential plus a $1/L^2$ term) to infinity in an attempt to get the absolute potential is not likely to be accurate, as we do not know the longer-range shape of the slope. In Figure 1, we have plotted (as the solid black curve) the calculated potential (including the extrapolation), with an additional -0.02 eV offset, over the range of distances for which we have measured the solvation potential slope. We chose the -0.02 eV offset of the simple integral of the determined solvation potential gradient to match the right edges of the Born model calculations for $\varepsilon_2 = 100$ (red curves in Figure 1). It can be seen that the whole determined potential curve closely follows the $\varepsilon_2 = 100$ Born model even up to ~1 ML away with only small deviations. It is expected that the potential is symmetric on both sides of any water film, and over the range of 1 to 10 ML away, independent of the water film thickness (when the potential is measured from the water's edge). The determined solvation potential for a 1.8 nm water film was reflected onto the opposite side of the film, as shown in Figure 1. We did not determine the potential minimum here, but following the previous work,[6] we expect it to be somewhere between the Born model curves for dielectric constants of 5 and 100. Somewhat arbitrarily, we have joined the two measured potential halves (assuming that the potential is symmetric about the water film) with a plausible well depth that is intermediate between these two sets of Born calculations ($\varepsilon_2 = 5$ and 100). This is shown in gray and is speculative (though consistent with our earlier estimates[6]).

The experimentally determined portion of the potential (in black) has a rather different shape than the curve for the $\varepsilon_2 = 5$ Born model: no offset allows the experimental curve to closely match the dashed green curve, despite the fact that the latter gives a fair estimate of the well depth. This was initially surprising. But for a "k-dependent" dielectric constant, this would be as predicted.[7] The solvation-energy well depth depends strongly upon the ability to optimally reorient the water molecules at close range to the ion. Of course, at that range, the continuum model does not accurately mimic the geometrical constraints of the hydrogen-bonding network within liquid water, but some of those constraints can be included by an extension of the continuum model. In a Fourier expression, the solvation potential for $L < 1$ ML (needed for a well depth estimate) would involve the behavior of ε at large k. The longer-range part of the solvation potential that we measured here depends on the small-k values of ε. Thus, our slope measurements are fit well with $\varepsilon_2 = 100$ while the well depth estimates require $\varepsilon_2 = 5$. The Born calculations for a water dielectric constant of 100 and 0.15−3.0 nm thick water films are shown as the red curves in Figure 1. These calculations reveal two important details. The first is that the right sides of all of the calculated curves are nearly identical at distances greater than 1 ML (0.42 nm) from the water films' right edges. This is consistent with our experimental observation that the solvation potential slope at these distances does not change with water film thickness. The second point is that the potential to the right of the water layer for a dielectric constant of 100 matches the shape of the experimentally determined potential fairly well.

We note that we did a few parallel experiments using hydronium (D_3O^+) instead of Cs^+ ions. The conditions and repetitions of the hydronium data were not sufficient for us to report quantitatively the solvation potential for hydronium ions. Without presenting any of the data, we do report that at least qualitatively we saw similar behavior. The movement of the hydronium ions within the films was similar to that observed for the Cs^+ cases, in that some hydronium ions escaped and some got trapped upon warming. In the hydronium case, the amount of trapped charge appeared to be substantially different than for the Cs^+ case. This may indicate that at that distance the hydronium solvation potential is different than the Cs^+ potential. Even for a simple Born model, this could happen, as the effective ion sizes should differ. It might also indicate a limited mobility for the hydronium (or Cs^+) ions that might allow the distances of the two ions from the water's edge to be different. Regardless, it appears that the detailed potential for hydronium could also be determined via more experiments.

Relevance. The ability to directly measure the chemical potential of an ion near an interface has applications to several topics of current interest, namely: (1) transport and "presentation" in multiphase chemistry and (2) potentials of mean force for ion transport in biological systems and in protein folding. Multiphase chemistry, such as that occurring between two immiscible liquids or in trace-gas interactions with atmospheric liquid aerosols, often only occurs if ions can cross over the interface or approach it to be in direct contact with the other phase. Thus, the interfacial solvation potential (or the closely related "potential of mean force")[1,21,22] controls both the kinetics and the static concentration of ions at the interface. In the last 10 years with increasing success, theory has addressed these issues.[21] The experimental confirmations of the theory are limited in detail. Our measurements of the ion potential at the oil−water interface are the most direct to date. Since we can easily modify the system (e.g., by using alcohols instead of water, using polar organics or different hydrocarbons, using more complex layerings, etc.), our approach permits many detailed tests of theory.

An important application of theory is in estimating the forces near bio-organics (such as proteins and cell walls) and inside ion channels, in order to predict the transport of ions near and through them, protein folding, and the like.[22] While our system is clearly planar and most of the biological systems are not, it is still possible to create complex planar interfaces with water, oils, and amino acids (for example) that would still be good tests of the new computational abilities, as we can determine the potential of mean force near them.

One pervasive notion about water, derived from numerous observations, is that near low-dielectric interfaces or for very thin films of water, or for the water nearest a metal substrate, the dielectric constant is greatly reduced compared with that of bulk water. Teschke, Ceotto, and De Souza[23] discuss some of these older measurements as well as a new measurement via atomic force microscopy. They assert that the water dielectric constant is decreased from the bulk value even at 10 nm from the interface and very strongly at 1 nm or less.[7] This has been applied, for example, to proton transport near biological membranes to predict a barrier to the approach of a hydronium ion toward the membrane on the order of 120 meV.[4,5] We find here (using a Born model) that our water film seems to have a high dielectric constant at distances from it (on the oil side) as short as two oil molecules (~0.7 nm) away and that the water film has this high dielectric constant (measured from the oil side) whether that water layer is two, three, or many molecular layers thick. We suggest that interfacial water usually has a high dielectric constant, similar to that of bulk water. Sometimes it may seem to have a low dielectric constant, when forced to respond in a way that requires specific short-range motions, such as when one uses concentrated ionic solutions (or high electrochemical potentials) to make for very short-range double layers. In such cases, the water responds as if it had a small dielectric constant, consistent with a k-dependent ε, because of the spatial detail required.[7] This k-dependent ε was considered in at least one paper as relevant to biological proton transport.[5]

Conclusions

The measurement of the solvation potential at the oil−water interface over distances of 0.4−4 nm of intervening 3MP is unique in its directness and its bridging of molecular to semimacroscopic distances. The numerical results, which were in general accord with expectations, are not directly surprising. However, it is reassuring that concepts used to fit single-ion solvation energies or the capacitance of 1 or 2 ML of water at electrode surface "double layers" work so well in understanding much of our results, giving one more confidence in applying them to a broader range of phenomena. We hope to use these and additional results to test ideas about k-dependent dielectric responses.[7] In principle, a full analysis of the results shown here, and of previous results without spacers,[6] may give a complete picture of the potential slope and its water-thickness-dependent minimum. However, this would require a full molecular dynamics treatment of the waters as discrete molecules and is beyond the scope of the current paper.

Acknowledgment. This research was performed in the Environmental Molecular Sciences Laboratory (EMSL), a national scientific user facility sponsored by the Department of Energy's Office of Biological and Environmental Research (OBER) and located at Pacific Northwest National Laboratory. This work was supported by a DOE/BES Chemical Sciences Grant and DOE/OBER (EMSL support).

JA805962X

(21) Jungwirth, P.; Winter, B. *Annu. Rev. Phys. Chem.* **2008**, *59*, 343–366.

(22) Allen, T. W.; Anderson, O. S.; Roux, B. *Biophys. Chem.* **2006**, *124*, 251–267.

(23) Teschke, O.; Ceotto, G.; de Souza, E. F. *Phys. Rev. E* **2008**, *64*, 011605.